Received: 13 April 2022 | Revised: 1 May 2022 | Accepted: 6 May 2022

DOI: 10.1111/hepr.13793

ORIGINAL ARTICLE

Hepatology Research

Comparison of modified CEUS LI-RADS with sonazoid and CT/MRI LI-RADS for diagnosis of hepatocellular carcinoma

Katsutoshi Sugimoto[1] | Kazuhiro Saito[2] | Natsuhiko Shirota[2] | Naohisa Kamiyama[3] | Kentaro Sakamaki[4] | Hiroshi Takahashi[1] | Takuya Wada[1] | Tatsuya Kakegawa[1] | Yusuke Tomita[1] | Masakazu Abe[1] | Yu Yoshimasu[1] | Hirohito Takeuchi[1] | Takao Itoi[1]

[1]Department of Gastroenterology and Hepatology, Tokyo Medical University, Tokyo, Japan

[2]Department of Radiology, Tokyo Medical University, Tokyo, Japan

[3]Ultrasound General Imaging, GE Healthcare, Hino, Tokyo, Japan

[4]Center for Data Science, Yokohama City University, Yokohama, Japan

Correspondence

Katsutoshi Sugimoto, Department of Gastroenterology and Hepatology, Tokyo Medical University, 6-7-1 Nishishinjuku, Shinjuku-ku, Tokyo 160-0023, Japan
Email: sugimoto@tokyo-med.ac.jp

Funding information

Tokyo Medical University Cancer Research Foundation (2021)

Abstract

Aim: To compare the diagnostic performance based on the modified CEUS Liver Imaging Reporting and Data System (LI-RADS), which includes Kupffer-phase findings as a major imaging feature, with that of CT and MRI (CT/MRI) LI-RADS for liver nodules in patients at high risk of HCC.

Methods: A total of 120 patients with 120 nodules were included in this retrospective study. The median size of the lesions was 20.0 mm (interquartile range, 14.0–30.8 mm). Of these lesions, 90.0% (108 of 120) were confirmed as HCCs, 6.7% (8 of 120) were intrahepatic cholangiocarcinomas, 1.7% (2 of 120) were metastases, and 1.7% (2 of 120) were dysplastic nodules. All nodules were diagnosed histopathologically. Each nodule was categorized according to the modified CEUS LI-RADS and CT/MRI LI-RADS version 2018. The diagnostic performance and inter-modality agreement of each criterion was compared.

Results: The inter-modality agreement for the modified CEUS LI-RADS and CT/MRI LI-RADS was slight agreement (kappa = 0.139, $p = 0.015$). The diagnostic accuracies of HCCs for the modified CEUS LR-5 and CT/MRI LR-5 were 70.0% (95% confidence interval [CI]: 61.0%, 78.0%) versus 70.8% (95% CI: 61.8%, 78.8%) ($p = 0.876$), respectively. The diagnostic accuracies of non-HCC malignancies for the modified CEUS LR-M and CT/MRI LR-M were 84.2% (95% CI: 76.4%, 90.2%) versus 96.7% (95% CI: 91.7%, 99.1%) ($p = 0.002$), respectively.

Conclusions: The diagnostic performance for HCCs on the modified CEUS LR-5 and CT/MRI LR-5 are comparable. In contrast, CT/MRI LR-M has better diagnostic performance for non-HCC malignancy than that of the modified CEUS LR-M.

KEYWORDS

contrast media, hepatocellular carcinoma, LI-RADS, sonazoid, ultrasound

Abbreviations: CEUS, Contrast-Enhanced Ultrasound; CI, Confidence interval; DN, Dysplastic nodule; EOB-MRI, Gadoxetic acid-enhanced magnetic resonance imaging; HCC, hepatocellular carcinoma; ICC, Intrahepatic cholangiocarcinoma; LI-RADS, Liver Imaging Reporting and Data System.

INTRODUCTION

Hepatocellular carcinoma (HCC) is the only type of cancer diagnosed noninvasively in high-risk patients based on typical imaging features of CT, MRI, or contrast-enhanced ultrasound (CEUS) often without biopsy.[1,2] Because many methods of imaging diagnostic criteria have been proposed, this may lead to some confusion among radiologists, hepatologists, and surgeons, who are responsible for the management of patients at risk for or with HCC.

Recently, to overcome the situation, the American College of Radiology developed the Liver Imaging Reporting and Data System (LI-RADS) at CT or MRI in patients at risk for HCC in 2011,[3] which has been refined and updated to version 2018.[4] In contrast, CEUS has unique advantages over CT and MRI, since it offers pure vascular images, real-time dynamic images, and excellent safety for patients with impaired renal function or allergies to iodine or gadolinium.[5] American College of Radiology (ACR) also established the CEUS LI-RADS in 2016[6] and further revised it in 2017.[7] Comparison between CT/MRI LI-RADS and CEUS LI-RADS for categorization has been previously performed and reported.[8–10]

The US contrast agents currently available are categorized into two types: pure blood pool contrast agents, such as Lumason (Bracco Diagnostics, Monroe Township, NJ, USA) and Definity (Lantheus Medical Imaging, Billerica, MA, USA) and combined blood pool and Kupffer cell contrast agents, such as Sonazoid (GE Healthcare, Oslo, Norway). Unfortunately, the current version of CEUS LI-RADS (version 2017) is applicable only to the pure blood pool contrast agents but not to the combined blood pool and Kupffer cell agents.

To overcome the gap those using Sonazoid in daily clinical practice (clinicians in many Asian countries, e.g.,), a modified CEUS LI-RADS that is also applicable to Sonazoid was developed.[11–13] The main difference between CEUS LI-RADS (version 2017) and the modified CEUS LI-RADS is that the former includes late and mild washout as a major imaging feature while the latter includes Kupffer-phase hypoenhancement as a major imaging feature.

To the best of our knowledge, there has been no report to compare CT/MRI LI-RADS and the modified CEUS LI-RADS. Thus, the purpose of this study was to compare CT/MRI LI-RADS version 2018 and the modified CEUS LI-RADS for the categorization performance for patients at high risk of HCC.

MATERIALS AND METHODS

This study was reviewed and approved by the Tokyo Medical University ethics review board. The requirement to obtain written informed consent was waived for this retrospective study.

Patients

A clinical/pathological database was used to retrospectively identify patients with risk factors for HCC who underwent contrast-enhanced CT (CECT) or gadoxetic acid (Gd-EOB-DTPA) enhanced MRI, abbreviated as EOB-MRI, and CEUS at our institution between March 2017 and December 2021 (Figure 1). Liver histology, including US-guided biopsy and surgical pathology, served as the standard reference. If the patients had multiple nodules, only one nodule which was histopathologically diagnosed was included. The inclusion criteria were (1) age 20 years or older; (2) nodules detected by CECT/EOB-MRI and US; (3) nodules with pathological diagnosis; and (4) an interval of less than 4 weeks between CECT/EOB-MRI and CEUS examinations. The patients with the following criteria were excluded: (1) cirrhosis due to a vascular disorder such as Budd-Chiari syndrome

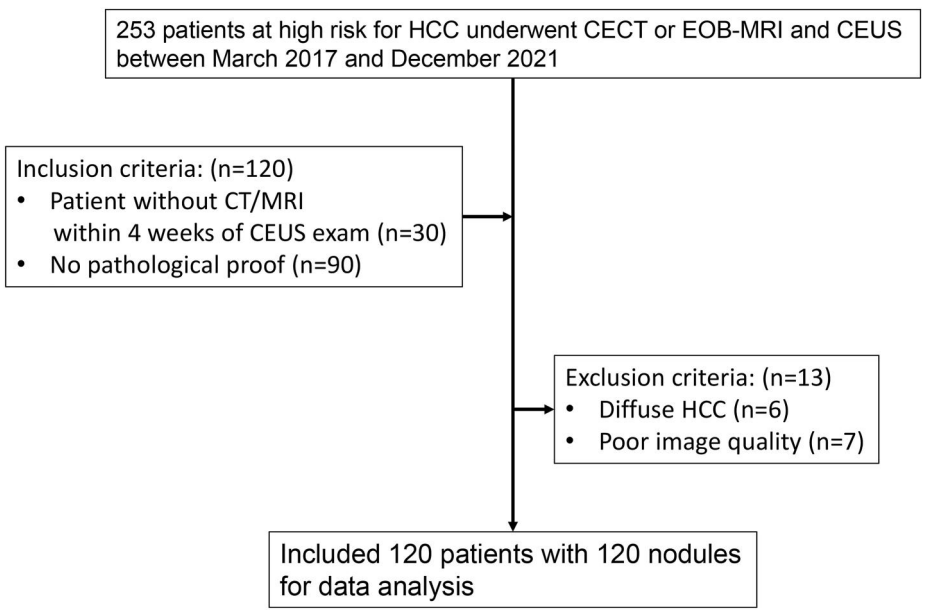

FIGURE 1 Flow diagram of study

or cardiac congestion; (2) diffuse HCC; and (3) poor image quality for any reason.

CEUS

US images were obtained by an Aplio i800 diagnostic US system (Canon Medical Systems, Otawara, Tochigi, Japan) equipped with a 3.5 MHz convex transducer (PVT-475BT), pulse inversion harmonic imaging mode, mechanical index 0.14–0.2 and a dynamic range of 45 dB, or by a LOGIQ E10 diagnostic US system (GE Healthcare, Wauwatosa, WI, USA) equipped with a 3.5 MHz convex transducer (C1-6-D), amplitude modulation imaging mode, mechanical index 0.16–0.2 and a dynamic range of 63 dB. If the lesion was observed with poor conspicuity on B-mode US, the fusion imaging technique of CT/MRI with US was used. The size, location and echogenicity of lesions were assessed. The second-generation US contrast agent Sonazoid (GE Healthcare) was injected as a 0.5-ml bolus into an antecubital vein via a 21-gauge peripheral intravenous cannula, followed by a 10-ml saline flush at a rate of 1.0-ml/s using a dedicated injector (Sonazoid Shot: Nemoto, Bunkyo-ku, Tokyo, Japan). A timer was started at the time of contrast agent injection. Images were recorded continuously as a cine clip for a period of 60 s immediately after injection of the contrast agent (for evaluation of the vascular phase), after which the scan was frozen. After a waiting period of approximately 10 min from the time of contrast agent injection to permit pooling of the agent in the liver parenchyma, enhancement of the lesion was observed using a sweep scan and images were recorded (for evaluation of the Kupffer phase or post-vascular phase). If missed to assess arterial phase enhancement in the first injection of Sonazoid, we performed another contrast injection in the Kupffer phase (i.e., "defect reperfusion imaging") to ensure whether arterial hyperenhancement or not. The sequence that was followed in the CEUS protocol is shown elsewhere.[11] The examination was performed by three hepatologists with more than 5 years of CEUS experience.

CT

CT was performed with 64 or 256 multidetector CT. Iodine contrast media with a concentration of 600 mgI/kg was injected through the antecubital vein during 30 s. Timing of the arterial phase was determined by monitoring the scan. The arterial phase scan was started at 20 s after reaching more than 100 HU in the abdominal aorta. The portal phase was 20 s after the arterial phase, and the equilibrium phase was 180 s after the arterial phase.

MRI

MRI was performed with 3T MRI system (MAGNETOM Vida or MAGNETOM Skyra, Siemens, Erlangen, Germany). T1-weighted images (T1WI) included in-phase and opposed-phase images. The T1WI parameters (in-phase and opposed-phase) were as follows: TR/TE, 4.2/2.57, 1.34 msec; flip angle, 10°; 1 averaging; matrix, 320 × 168; parallel acquisition technique (PAT) factor 3 with a generalized autocalibrating partially parallel acquisition (GRAPPA) algorithm; slice thickness, 2 mm and acquisition time, 18 s. Fat-suppressed respiratory-triggered T2-weighted images parameters were as follows: TR/TE, 3840/85 msec; flip angle, 100°; echo train length, 28; matrix, 320 × 320; slice thickness, 5 mm; 1 averaging; and PAT factor 3 with the GRAPPA algorithm. Diffusion weighted images (DWI) were obtained under free breath. DWI parameters were as follows: TR/TE, 6600/46 msec; flip angle, 90°; matrix, 360 × 460; slice thickness, 5 mm; 3 averaging and b-values 200 and 800 s/mm^2.

A total of 0.025 mmol/kg of Gd-EOB-DTPA was injected via the antecubital vein at a rate of 2 ml/sec, followed by 40 ml of physiological saline. A three-dimensional (3D) volumetric interpolated breath-hold examination (3D-VIBE) was performed. The 3D-VIBE parameters were as follows: TR/TE, 2.8/0.93 msec; flip angle, 9°; matrix, 480 × 248; PAT factor, 2; slice thickness, 3 mm; and acquisition time, 20 s. A monitoring scan technique (the Care Bolus method) was used to obtain the optimal arterial phase. In addition to a pre-contrast acquisition, the dynamic datasets covered the arterial phase with acquisitions at 9 and 19 s after contrast media arriving at aortic arch. The portal phase and hepatobiliary phase images were obtained at 70 s and 20 min respectively. In addition, an acquisition was obtained at 240 s after injection of contrast agent.

CEUS imaging assessment

One hepatologist with more than 15 years of experience in liver CEUS, who was blinded to the reference standard results and other imaging findings for the liver nodules, reviewed the CEUS examinations and assigned each nodule to a category according to the modified CEUS LI-RADS,[11,12] which is based on CEUS LI-RADS (2017 version).[14] Briefly, the main difference between CEUS LI-RADS (2017 version) and the modified CEUS LI-RADS is that former includes late and mild washout as a major imaging feature, while the latter includes Kupffer phase findings as a major imaging feature. The other criteria in the modified CEUS LI-RADS are the same as those in CEUS LI-RADS (2017 version).[14]

CT/MRI imaging assessment

One radiologist with more than 9 years of experience in liver CT/MRI, who was blinded to the reference standard results and other imaging findings for the liver nodules, reviewed the CT/MRI examinations and assigned each nodule to a category according to the CT/RMI LI-RADS (2018 version).[15] For patients who received both CECT

and EOB-MRI examinations, the nodules were classified according to EOB-MRI.

Statistical analysis

Qualitative data are presented as numbers and percentages, and quantitative data are presented as median and interquartile range (IQR). The per-lesion sensitivity, specificity, positive predictive value (PPV), negative predictive value (NPV), and accuracy with the 95% confidence interval (CI) of both the modified CEUS LI-RADS and CT/RMI LI-RADS (2018 version) were compared by using the McNemar test. Categorical variables were compared using the paired chi-square test. The Cohen's kappa coefficient was used for the evaluation of inter-modality agreement. All statistical analyses were performed using SAS software, version 9.4 (SAS Institute). Values of $p < 0.05$ were considered as statistically significant.

TABLE 1 Baseline characteristics

Characteristics	Value
No. of patients	120
Median age (y)[a]	73 (67–80)
Sex	
Male	90
Female	30
Presence of cirrhosis	96 (80.0%)
Liver disease etiology	
HCV	41 (34.2%)
Alcohol	33 (27.5%)
HBV	30 (25.0%)
NASH	14 (11.7%)
AIH	2 (1.7%)
No. of lesions	120
Lesion size (mm)[a]	20.0 (14.0–30.8)
Diagnosis method	
Biopsy	112 (93.3%)
Surgery	8 (6.7%)
Histopathologic analysis	
HCC	108 (90.0%)
Well-differentiated	31 (28.7%)
Moderately differentiated	65 (60.2%)
Poorly differentiated	12 (11.1%)
ICC	8 (6.7%)
Metastasis	2 (1.7%)
DN	2 (1.7%)

Abbreviations: AIH, autoimmune hepatitis; DN, dysplastic nodule; HBV, hepatitis B virus; HCC, hepatocellular carcinoma; HCV, hepatitis C virus; ICC, intrahepatic cholangiocarcinoma; NASH, non-alcoholic steatohepatitis; y, year.

[a]Data in parentheses are interquartile range.

RESULTS

Patients and liver nodule characteristics

A total of 120 patients 120 nodules (male: 90, female: 30; median age and interquartile range; 73 years and 67–80 years) were finally included in this study. The median size of the lesions was 20.0 mm (interquartile range, 14.0–30.8 mm). Of these lesions, 90.0% (108 of 120) were confirmed as HCCs including 28.7% (31 of 108): well-differentiated HCC; 60.2% (65 of 108): moderately differentiated HCC; 11.1% (12 of 108): poorly differentiated HCC, 6.7% (8 of 120) were intrahepatic cholangiocarcinomas (ICCs), 1.7% (2 of 120) were metastases, and 1.7% (2 of 120) were dysplastic nodules. A total of 112 nodules were confirmed by biopsy and 8 nodules were confirmed by surgical pathology. The most common cause of liver disease was hepatitis C virus infection (34.2% [41 of 120], and 80.0% (90 of 120) of participants had cirrhosis. The clinical and pathologic characteristics of the participants and the targeted nodules are described in Table 1.

Distribution of the modified CEUS LI-RADS and CT/MRI categories

The percentages of nodules in LR-3, LR-4, LR-5, and LR-M for the modified CEUS LI-RADS were 9.2%, 6.7%, 61.7%, and 22.5%, and for CT/MRI LI-RADS, 6.7%, 20.8%, 60.8%, and 11.7%, respectively (Table 2) and the distributions were different form each other ($p < 0.0001$). Inter-modality agreement for the modified CEUS LI-RADS and CT/MRI LI-RADS was slight agreement (kappa = 0.139 [95%CI: 0.003, 0.275], $p = 0.015$). The results of classification by the modified CEUS LI-RADS and CT/MRI LI-RADS for the nodules and pathological diagnosis are shown in Table 3 and the distributions were also different form each other ($p < 0.0001$).

TABLE 2 Comparison between CEUS and CT/MRI classification

CEUS ($n = 120$) category	CT ($n = 52$)/MRI ($n = 68$) category				
	3	4	5	M	Total
3	2 (2)	8 (7)	1 (1)	0	11 (10)
4	0	3 (2)	5 (5)	0	8 (7)
5	6 (6)	13 (13)	53 (53)	2 (1)	74 (73)
M	0	1 (1)	14 (14)	12 (3)	27 (18)
Total	8 (8)	25 (23)	73 (73)	14 (4)	120 (108)

Note: Data in parentheses are number of HCCs.

Modified CEUS LI-RADS and CT/MRI LI-RADS categories and degree of histopathologic differentiation of HCC

The relationship between the modified CEUS LI-RADS categories and the degree of HCC differentiation and between the CT/MRI LI-RADS categories and the degree of HCC differentiation are shown in Table 4. On the modified CEUS LI-RADS categories, all poorly differentiated HCCs were classified as LR-M, resulting in a statistically significant difference among the distribution. In contrast, there was no statistically significant difference among the distribution on the CT/MRI LI-RADS categories.

The diagnostic performance of the modified CEUS LI-RADS and CT/MRI LI-RADS

The diagnostic performances for HCCs of the modified CEUS LI-RADS and CT/MRI LI-RADS are shown in Table 5. The sensitivities for the modified CEUS LR-5 and CT/MRI LR-5 were 67.6% (95% CI: 57.9%, 76.3%) versus 67.6% (95% CI: 57.9%, 76.3%) (p = 1.000); the specificities were 91.7% (95% CI: 61.5%, 99.8%) versus 100% (95% CI: 64.0%, 100%); the PPVs were 98.6% (95% CI: 97.2%, 100%) versus 100% (95% CI: 92.7%, 100%); the NPVs of HCCs were 23.9% (95% CI: 12.6%, 38.8%) versus 25.5% (95% CI: 13.9%, 40.3%); and the accuracies were 70.0% (95% CI: 61.0%, 78.0%) versus 70.8% (95% CI: 61.8%, 78.8%) (p = 0.876), respectively. However, some of these p-values could not be calculated because the Hessian matrix was not positive, likely due to the imbalance between number of HCCs and others.

The diagnostic performances for non-HCC malignancies of the modified CEUS LI-RADS and CT/MRI LI-RADS are also shown in Table 5. The sensitivities for the modified CEUS LR-M and CT/MRI LR-M were 90.0% (95% CI: 55.5%, 99.7%) versus 100% (95% CI: 58.7%, 100%); the specificities were 83.6% (95% CI: 75.4%, 90.0%) versus 96.4% (95% CI: 91.0%, 99.0%) (p = 0.001); the PPVs were 33.3% (95% CI: 16.5%, 54.0%) versus 71.4% (95% CI: 41.9%, 91.6%); the NPVs of HCCs were 98.9% (95% CI: 94.2%, 100%) versus 100% (95% CI: 94.9%, 100%); and the accuracies were 84.2% (95% CI: 76.4%, 90.2%) versus 96.7% (95% CI: 91.7%, 99.1%) (p = 0.002), respectively. However, some of these p-values could not be calculated because the Hessian matrix was not positive, likely due to the imbalance between number of HCCs and others.

TABLE 3 Comparison of histopathologic results and category between CEUS and CT/MRI

Category	CEUS (n = 120)					CT (n = 52)/MRI (n = 68)				
Pathology	3	4	5	M	Total	3	4	5	M	Total
HCC	10	7	73	18	108	8	23	73	4	108
ICC	0	0	1	7	8	0	0	0	8	8
Metastasis	0	0	0	2	2	0	0	0	2	2
DN	1	1	0	0	2	0	2	0	0	2
Total	11	8	74	27	120	8	25	73	14	120

Abbreviations: DN, dysplastic nodule; HCC, hepatocellular carcinoma; ICC, intrahepatic cholangiocarcinoma.

DISCUSSION

Our study results demonstrated that both the modified CEUS LR-5 and CT/MRI LI-RADS had a high specificity (91.7% and 100%) and PPV (98.6%, 100%) for the diagnosis of HCC, respectively. In contrast, the result of this study showed that the inter-modality agreement for the LI-RADS category between CEUS and CT/MRI was slight agreement (kappa = 0.139). This means that CEUS and CT/MRI may see different characteristic features on HCC. Thus, both CEUS and CT/MRI should be necessary for diagnosing HCC correctly.

The discordance between CEUS and CT/MRI for LR-3 was analyzed in this study. LR-3 is assigned to findings that have an intermediate malignant probability. In this study, 10 HCCs were classified as the modified CEUS LR-3, among which only 1 HCC was reclassified as CT/RMI LR-5. In contrast, 8 HCCs were classified as CT/MRI LR-3, among which 6 HCCs were reclassified as the modified CEUS LR-5 (Figure 2). We can attribute this improvement in the superiority of CEUS to detect arterial phase hyperenhancement

TABLE 4 Comparison of histopathologic differentiation of HCC and category between CEUS and CT/MRI

Category	CEUS (n = 120)					CT (n = 52)/MRI (n = 68)				
Histopathologic differentiation of HCC	3	4	5	M	Total	3	4	5	M	Total
Well-differentiated	9	4	18	0	31	4	11	15	1	31
Moderately differentiated	1	3	55	6	65	4	11	48	2	65
Poorly differentiated	0	0	0	12	12	0	1	10	1	12
Total	10	7	73	18	108	8	23	73	4	108

Abbreviation: HCC, hepatocellular carcinoma.

CEUS: $p < 0.0001$.

CT/MRI: Not significant

TABLE 5 Comparison of diagnostic performance of LR-5 and LR-M categories between CEUS and CT/MRI

	HCC			Non-HCC malignancy		
Variable	**CEUS LR-5**	**CT/MRI LR-5**	***p* value**	**CEUS LR-M**	**CT/MRI LR-M**	***p* value**
Sensitivity (%)	67.6	67.6	1.000[a]	90.0	100.0	n.c[a]
	73/108 (57.9, 76.3)	73/108 (57.9, 76.3)		9/10 (55.5, 99.7)	10/10 (58.7, 100.0)	
Specificity (%)	91.7	100.0	n.c[a]	83.6	96.4	0.001[a]
	11/12 (61.5, 99.8)	12/12 (64.0, 100.0)		92/110 (75.4, 90.0)	106/110 (91.0, 99.0)	
PPV (%)	98.6	100.0	n.c [a]	33.3	71.4	n.c[a]
	73/74 (97.2, 100.0)	73/73 (92.7, 100.0)		9/27 (16.5, 54.0)	10/14 (41.9, 91.6)	
NPV (%)	23.9	25.5	n.c[a]	98.9	100.0	n.c[a]
	11/46 (12.6, 38.8)	12/47 (13.9, 40.3)		92/93 (94.2, 100.0)	106/106 (94.9, 100.0)	
Accuracy (%)	70.0	70.8	0.876[a]	84.2	96.7	0.002[a]
	84/120 (61.0, 0.780)	85/120 (61.8, 78.8)		101/120 (76.4, 90.2)	116/120 (91.7, 99.1)	

Note: Data in parentheses are 95% confidence interval.

Abbreviations: HCC, hepatocellular carcinoma; n.c, not calculated; NPV, negative predicted value; PPV, positive predicted value.

[a]McNemar test.

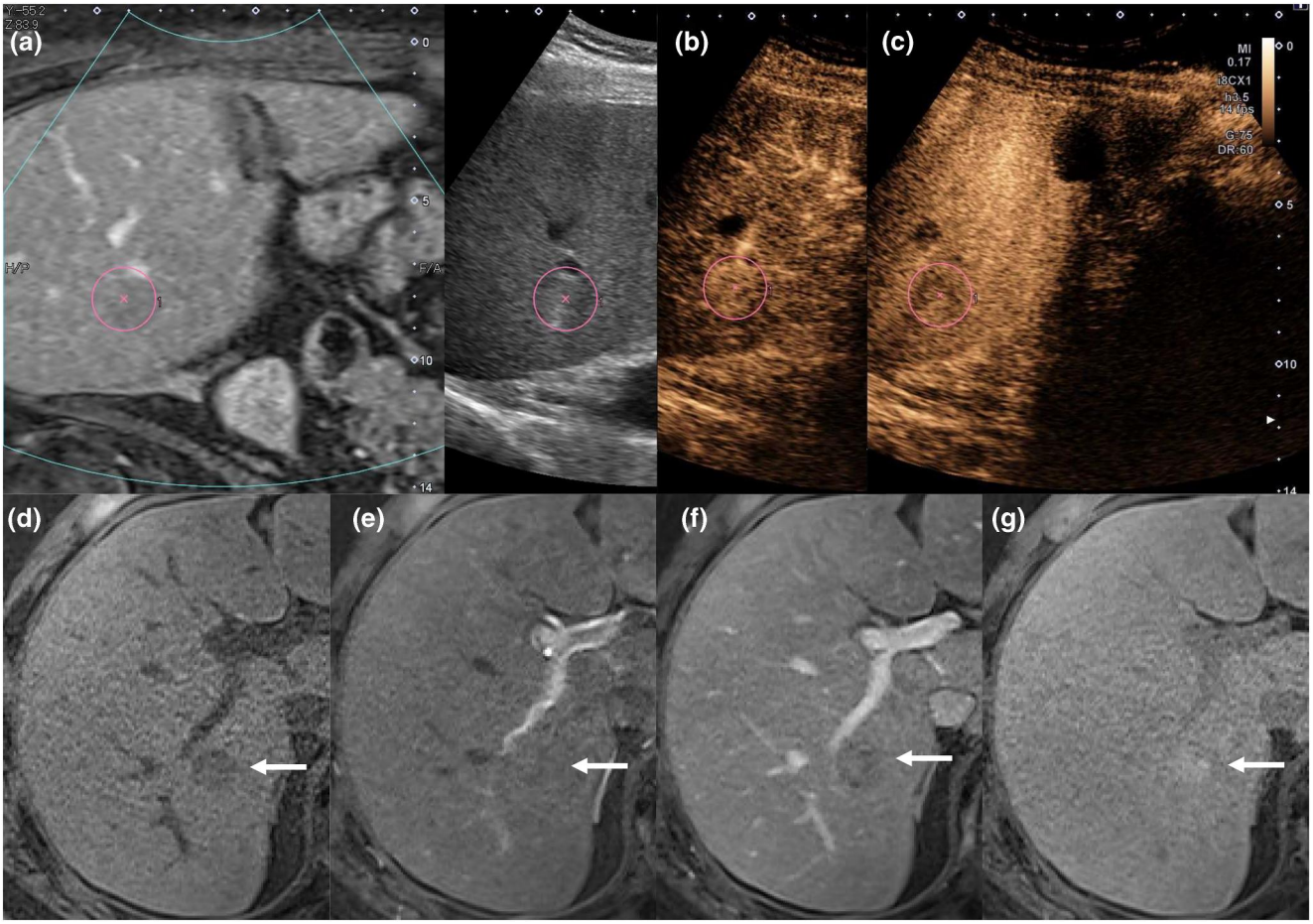

FIGURE 2 A moderately differentiated HCC in S7 is categorized as the modified CEUS LR-5 and CT/MRI LR-3 by EOB-MRI in a 70-year-old man with alcoholic cirrhosis. (a, pink circle) B-mode US image with portal-venous phase EOB-MRI fusion image shows 2.0-cm ill-defined observation. CEUS: (b, pink circle) shows arterial phase hyper enhancement, (c, pink circle) followed by hypo-enhancement in 10 minutes after contrast injection, or Kupffer phase. EOB-MRI: (d, arrow) shows hypo-intense in the pre-contrast T1 weighted image, (e, arrow) shows iso-enhancement in the arterial phase, (f, arrow) washout in the portal venous phase, (g arrow) hyper-intense in the hepato-biliary phase

(APHE) compared to that of CT or MRI.[16] Thus, for CT/MRI LR-3 and LR-4 nodules which show no APHE, CEUS examination should be performed to ensure whether those nodules are truly hypo-vascular or not.

The discordance CEUS and CT/MRI for LR-M was also analyzed in this study. LR-M is assigned to findings that are probably or definitely malignant but not HCC specific. In this study, 27 nodules were classified as the modified CEUS LR-M, among which 18 nodules (67%; 18/27) were histopathologically diagnosed as HCCs (Figure 3). In contrast, 14 nodules were classified as CT/MRI LR-M, among which only 4 nodules (29%; 4/14) were histopathologically diagnosed as HCCs. Accordingly, compared with the modified CEUS LR-M, CT/MRI LR-M had higher diagnostic performance for non-HCC malignancies. The main reason for this was that some HCCs were more likely to

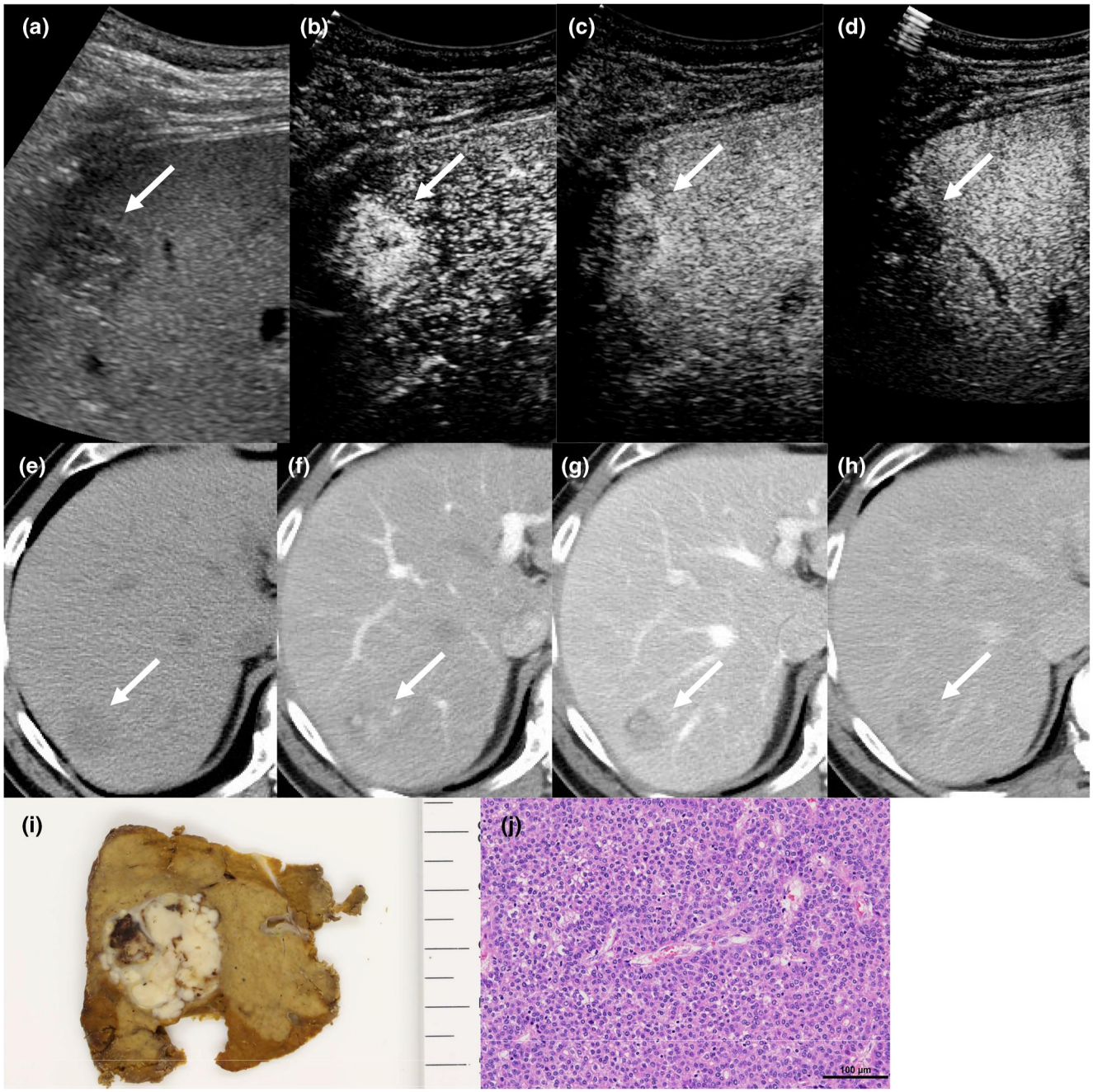

FIGURE 3 A poorly differentiated HCC in S7 is categorized as the modified CEUS LR-M and CT/MRI LR-5 by CECT in a 71-year-old man with alcoholic cirrhosis. (a, arrow) B-mode US image shows 2.7-cm hypo-echoic observation. CEUS: (b, arrow) shows arterial phase hyper enhancement, (c, arrow) followed by washout at 42 s after contrast agent injection, (d, arrow) contrast defect in 10 minutes after contrast injection, or Kupffer phase. (e, arrow) Pre-contrast CT image shows hypo-dense observation. CECT: (f, arrow) shows arterial phase hyper enhancement, (g, arrow) washout in the portal venous phase, (h, arrow) washout in the delayed phase. (i) Grossly, the HCC presents as a simple nodular type with extranodular growth. (j) The HCC shows solid growth pattern (HE, × 200)

present an enhancement pattern of "early washout" on CEUS. Moreover, these nodules which showed early washout on CEUS were composed of 12 poorly differentiated HCCs (100%; 12/12), six moderately differentiated HCCs (9.2%; 6/65) and no well-differentiated HCCs (0%; 0/31). In contrast, one poorly differentiated HCC was classified as CT/MRI LR-M.

Although the early washout feature on CEUS for poorly differentiated HCCs decreased the diagnostic performance of HCC, this finding is actually advantageous because poorly differentiated HCCs have higher malignant potential than other types of HCCs and are essentially similar to metastasis.[17,18] Thus, we recommend that in clinical practice when we encounter LR-M nodules on CEUS due to early washout, firstly we should perform CT or MRI to rule out the possibility of non-HCC malignancies and then the nodule was classified as CT/MRI LR-5, which has high probability of poorly differentiated HCC. In that case, we may take more radial therapy such as liver resection rather that local ablation therapy.[17,18]

In this study, we used the modified CEUS LI-RADS using Kupffer-phase hypoenhancement as a major imaging feature for LR-5 instead of using late phase mild washout. There may be concern about whether the hypoenhancement in Kupffer-phase findings can be used as an alternative to "washout". The same concern was raised for EOB-MRI about whether hypointensity observed in the hepatobiliary phase (HBP) findings can be used as an alternative to "washout" for the noninvasive diagnosis of HCC. In this regard, Joo et al. explored the question and demonstrated that the criterion of "hypointensity on the portal-venous-phase (PVP)" of EOB-MRI resulted in the high specificity of 97.9%, while the criteria of "hypointensity on the PVP and/or transitional phase (TP), and/or HBP" resulted in lower specificities of 86.3% and 48.4%, respectively. Thus, they concluded that washout should be assessed in the PVP alone rather than combined with the TP or HBP for a more specific diagnosis of HCC on EOB-MRI.[19] Based on this, EOB-MRI as well as CT and MRI using extracellular agents has been incorporated with CT/MRI LI-RADS in the same manner.

Does this also apply to Sonazoid? Takahashi et al. explored the question and demonstrated that after 5 min of Sonazoid injection, 38 out of 52 HCCs (73.1%) showed washout, while after 10 min, the so-called Kupffer-phase, 47 out of 52 HCCs (90.4%) showed washout, resulting in higher sensitivity and accuracy without reducing specificity when using Kupffer phase findings as major imaging feature. Thus, they concluded that washout should be assessed in the Kupffer phase.[12]

In this article, we addressed the usefulness of LI-RADS especially the modified CEUS LI-RADS. However, one question may arise: If Sonazoid-enhanced CEUS is applicable in Japan, will CEUS LI-RAD become widely used in Japan? CEUS LI-RADS may help standardize CEUS procedure and the classification of hepatic nodules in cirrhotic liver, facilitating communication between hepatologists, sonologists, radiologists, and surgeons. However, the feature of LI-RADS is to enhance specificity rather than sensitivity because liver transplantation is one of the major treatment options in Western countries. In contrast, since there are few liver transplants in Japan, high sensitivity is also required. Thus, in order for CEUS LI-LADS to become widely used in Japan, it may be necessary to revise CEUS LI-LADS and adapt it to Japanese medical care.

There are several limitations in the study: First, a prospective and multicenter study is needed to validate the inter-modality agreement and diagnostic performance between the modified CEUS LI-RADS and CT/MRI LI-RADS. Second, although all nodules in this study were diagnosed by histopathologically, almost all (93.3%) was made by needle biopsy and especially this may be concerned when diagnosing differentiation of HCCs. Third, the relatively small number of benign lesions and non-HCC malignancies hindered the generalization of our results. Fourth, CT and MRI were not analyzed separately due to the relatively small number of nodules. Finally, although we mentioned HCC is the only type of cancer diagnosed non-invasively in high-risk patients based on the typical imaging features of CT, MRI, or CEUS, we performed tumor biopsy as a routine clinical practice. It seems paradoxical, but we make it a rule to perform tumor biopsy with informed consent before percutaneous local ablation therapy to obtain pathological evidence, which may be acceptable especially in the academic center.

In conclusion, the modified CEUS LI-RADS criteria is reasonable for non-invasive diagnosis of liver nodules in patients at high risk of HCC. The modified CEUS and CT/MRI LR-5 corresponds to comparable positive predictive values of HCC. For LR-3 and LR-4 nodules categorized by CT/MRI, CEUS should be performed. CT/MRI LR-M has better diagnostic performance for non-HCC malignancies than the modified CEUS LR-M.

ACKNOWLEDGEMENTS

This study was supported by the Cancer Research Grant afforded by the Tokyo Medical University Cancer Research Foundation (2021).

CONFLICT OF INTEREST

The authors declare no conflict of interest.

ETHICAL STATEMENT

This study was reviewed and approved by the Tokyo Medical University ethics review board. The requirement to obtain written informed consent was waived for this retrospective study.

REFERENCES

1. Marrero JA, Kulik LM, Sirlin CB, Zhu AX, Finn RS, Abecassis MM, et al. Diagnosis, staging, and management of hepatocellular carcinoma: 2018 practice guidance by the American association for the study of liver diseases. Hepatology. 2018;68(2):723–50. https://doi.org/10.1002/hep.29913
2. Kudo M, Kawamura Y, Hasegawa K, Tateishi R, Kariyama K, Shiina S, et al. T management of hepatocellular carcinoma in Japan: JSH consensus statements and recommendations 2021 update. Liver Cancer. 2021;10(3):181–223. https://doi.org/10.1159/000514174
3. Mitchell DG, Bruix J, Sherman M, Sirlin CB. LI-RADS (liver imaging reporting and data system): summary, discussion, and consensus of the LI-RADS management working group and future directions. Hepatology. 2015;61(3):1056–65. https://doi.org/10.1002/hep.27304
4. Chernyak V, Fowler KJ, Kamaya A, Kielar AZ, Elsayes KM, Bashir MR, et al. Liver imaging reporting and data system (LI-RADS) version

2018: imaging of hepatocellular carcinoma in at-risk patients. Radiology. 2018;289(3):816–30. https://doi.org/10.1148/radiol.2018181494
5. Claudon M, Dietrich CF, Choi BI, Cosgrove DO, Kudo M, Nolsøe CP, et al. Guidelines and good clinical practice recommendations for contrast enhanced ultrasound (CEUS) in the liver--update 2012: a WFUMB-EFSUMB initiative in cooperation with representatives of AFSUMB, AIUM, ASUM, FLAUS and ICUS. Ultraschall der Med. 2013;34:11–29.
6. Kono Y, Lyshchik A, Cosgrove D, Dietrich CF, Jang HJ, Kim TK, et al. Contrast enhanced ultrasound (CEUS) liver imaging reporting and data system (LI-RADS®): the official version by the American College of Radiology (ACR). Ultraschall der Med. 2017;38(01):85–6. https://doi.org/10.1055/s-0042-124369
7. Wilson SR, Lyshchik A, Piscaglia F, Cosgrove D, Jang HJ, Sirlin C, et al. CEUS LI-RADS: algorithm, implementation, and key differences from CT/MRI. Abdom Radiol (NY). 2018;43(1):127–42. https://doi.org/10.1007/s00261-017-1250-0
8. Kim TK, Noh SY, Wilson SR, Kono Y, Piscaglia F, Jang HJ, et al. Contrast-enhanced ultrasound (CEUS) liver imaging reporting and data system (LI-RADS) 2017 - a review of important differences compared to the CT/MRI system. Clin Mol Hepatol. 2017;23(4):280–9. https://doi.org/10.3350/cmh.2017.0037
9. Caraiani C, Boca B, Bura V, Sparchez Z, Dong Y, Dietrich C. CT/MRI LI-RADS v2018 vs. CEUS LI-RADS v2017-can things Be put together? Biology. 2021;10(5):412. https://doi.org/10.3390/biology10050412
10. Ding J, Long L, Zhang X, Chen C, Zhou H, Zhou Y, et al. Contrast-enhanced ultrasound LI-RADS 2017: comparison with CT/MRI LI-RADS. Eur Radiol. 2021;31(2):847–54. https://doi.org/10.1007/s00330-020-07159-z
11. Sugimoto K, Kakegawa T, Takahashi H, Tomita Y, Abe M, Yoshimasu Y, et al. T usefulness of modified CEUS LI-RADS for the diagnosis of hepatocellular carcinoma using sonazoid. Diagnostics. 2020;10:828. https://doi.org/10.3390/diagnostics10100828
12. Takahashi H, Sugimoto K, Kamiyama N, Sakamaki K, Kakegawa T, Wada T, et al. Noninvasive diagnosis of hepatocellular carcinoma on sonazoid-enhanced US: value of the Kupffer phase. Diagnostics. 2022;12(1):141. https://doi.org/10.3390/diagnostics12010141
13. Hwang JA, Jeong WK, Min JH, Kim YY, Heo NH, Lim HK. Sonazoid-enhanced ultrasonography: comparison with CT/MRI Liver Imaging Reporting and Data System in patients with suspected hepatocellular carcinoma. Ultrasonography. 2021;40(4):486–98. https://doi.org/10.14366/usg.20120
14. American College of Radiology CEUS liver imaging reporting and data system version 2017. https://www.acr.org/Clinical-Resources/Reporting-and-Data-Systems/LI-RADS/CEUS-LI-RADS-v2017
15. American College of Radiology CT/MRI liver imaging reporting and data system version 2018. https://www.acr.org/Clinical-Resources/Reporting-and-Data-Systems/LI-RADS/CT-MRI-LI-RADSv2018
16. Sugimoto K, Moriyasu F, Shiraishi J, Saito K, Taira J, Saguchi T, et al. Assessment of arterial hypervascularity of hepatocellular carcinoma: comparison of contrast-enhanced US and gadoxetate disodium-enhanced MR imaging. Eur Radiol. 2012;22(6):1205–13. https://doi.org/10.1007/s00330-011-2372-3
17. Oishi K, Itamoto T, Amano H, Fukuda S, Ohdan H, Tashiro H, et al. Clinicopathologic features of poorly differentiated hepatocellular carcinoma. J Surg Oncol. 2007;95(4):311–6. https://doi.org/10.1002/jso.20661
18. Sasaki K, Matsuda M, Ohkura Y, Kawamura Y, Inoue M, Hashimoto M, et al. The influence of histological differentiation grade on the outcome of liver resection for hepatocellular carcinomas 2 cm or smaller in size. World J Surg. 2015;39(5):1134–41. https://doi.org/10.1007/s00268-014-2806-6
19. Joo I, Lee JM, Lee DH, Jeon JH, Han JK, Choi BI. Noninvasive diagnosis of hepatocellular carcinoma on gadoxetic acid-enhanced MRI: can hypointensity on the hepatobiliary phase be used as an alternative to washout? Eur Radiol. 2015;25(10):2859–68. https://doi.org/10.1007/s00330-015-3686-3

How to cite this article: Sugimoto K, Saito K, Shirota N, Kamiyama N, Sakamaki K, Takahashi H, et al. Comparison of modified CEUS LI-RADS with sonazoid and CT/MRI LI-RADS for diagnosis of hepatocellular carcinoma. Hepatol Res. 2022;1–9. https://doi.org/10.1111/hepr.13793